Published in final edited form as:

J Cell Physiol. 2019 September ; 234(9): 15048–15060. doi:10.1002/jcp.28146.

Trpm2 enhances physiological bioenergetics and protects against pathological oxidative cardiac injury: Role of Pyk2 phosphorylation

Barbara A. Miller[4], **JuFang Wang**[1], **Jianliang Song**[1], **Xue-Qian Zhang**[1], **Iwona Hirschler-Laszkiewicz**[4], **Santhanam Shanmughapriya**[1,3], **Dhanendra Tomar**[1,3], **Sudasan Rajan**[1,3], **Arthur M. Feldman**[2], **Muniswamy Madesh**[1,3], **Shey-Shing Sheu**[5], **Joseph Y. Cheung**[1,2]

[1]Center of Translational Medicine, Lewis Katz School of Medicine of Temple University, Philadelphia, PA 19140

[2]Department of Medicine, Lewis Katz School of Medicine of Temple University, Philadelphia, PA 19140

[3]Department of Biochemistry, Lewis Katz School of Medicine of Temple University, Philadelphia, PA 19140

[4]Department of Pediatrics, The Pennsylvania State University College of Medicine, Hershey, Pennsylvania 17033

[5]Center for Translational Medicine, Sidney Kimmel Medical College, Thomas Jefferson University, Philadelphia, Pennsylvania 19107.

Abstract

The mechanisms by which Trpm2 channels enhance mitochondrial bioenergetics and protect against oxidative stress induced cardiac injury remain unclear. Here, the role of proline-rich tyrosine kinase 2 (Pyk2) in Trpm2 signaling is explored. Activation of Trpm2 in adult myocytes with H_2O_2 resulted in 10- to 21-fold increases in Pyk2 phosphorylation in wild-type (WT) myocytes which was significantly lower (~40%) in Trpm2 knockout (KO) myocytes. Pyk2 phosphorylation was inhibited (~54%) by the Trpm2 blocker clotrimazole. Buffering Trpm2-mediated Ca^{2+} increase with BAPTA resulted in significantly reduced pPyk2 in WT but not in KO myocytes, indicating Ca^{2+} influx through activated Trpm2 channels phosphorylated Pyk2. Part of phosphorylated Pyk2 translocated from cytosol to mitochondria which has been previously shown to augment mitochondrial Ca^{2+} uptake and enhance ATP generation. Although Trpm2-mediated Ca^{2+} influx phosphorylated Ca^{2+}-calmodulin kinase II (CaMKII), the CaMKII inhibitor KN93 did not significantly affect Pyk2 phosphorylation in H_2O_2-treated WT myocytes. After ischemia/reperfusion (I/R), Pyk2 phosphorylation and its downstream pro-survival signaling molecules (pERK1/2 and pAkt) were significantly lower in KO-I/R when compared to WT-I/R hearts. After hypoxia/reoxygenation, mitochondrial membrane potential was lower and superoxide level

Address correspondence to: Joseph Y. Cheung, M.D., Ph.D., 3500 N. Broad Street, MERB 958, Philadelphia, PA 19140, Joseph.cheung@tuhs.temple.edu, Tel. 215-707-1799, Fax. 215-707-9890.

6. Conflict of Interests

None.

was higher in KO myocytes, and were restored to WT values by the mitochondria-targeted superoxide scavenger MitoTempo. Our results suggested that Ca^{2+} influx via tonically activated Trpm2 phosphorylated Pyk2, part of which translocated to mitochondria, resulting in better mitochondrial bioenergetics to maintain cardiac health. After I/R, Pyk2 activated pro-survival signaling molecules and prevented excessive increases in reactive oxygen species, thereby affording protection from I/R injury.

Keywords

voltage-independent Ca^{2+} channels; oxidative injury; mitochondrial oxidants; hypoxia-reoxygenation; ischemic cardiomyopathy

1. Introduction

Transient receptor potential (Trp) channels are involved in many fundamental cell functions and associated with many disease states (Nilius, Owsianik et al. 2007). Trpm channels are a subgroup of Trp channel superfamily. Trpm2 is expressed in many tissues including heart, vasculature, hematopoietic cells and brain (Hecquet, Ahmmed et al. 2008, Miller and Zhang 2011). Trpm2 is activated by adenosine diphosphate-ribose (ADPR) and H_2O_2 and mediates Ca^{2+} influx into the cell (Sumoza-Toledo and Penner 2011). Trpm2 has an essential role in susceptibility to oxidative stress (Sano, Inamura et al. 2001, Hara, Wakamori et al. 2002, Miller and Zhang 2011). The classical paradigm is that activation of Trpm2 induces cell death by sustained increases in intracellular Ca^{2+} concentration ($[Ca^{2+}]_i$) (Hara, Wakamori et al. 2002, Sumoza-Toledo and Penner 2011), or mediates enhanced chemokine production in hematopoietic cells thereby aggravating inflammatory response and tissue injury (Takahashi, Kozai et al. 2011). Quite unexpectedly, our recent data demonstrated that Trpm2 is essential in cellular bioenergetics maintenance in both the heart (Miller, Hoffman et al. 2014, Hoffman, Miller et al. 2015) and neuroblastoma cells (Chen, Hoffman et al. 2014); and that Trpm2 protects the heart (Miller, Wang et al. 2013, Hoffman, Miller et al. 2015) and neuroblastoma (Chen, Zhang et al. 2013) from oxidative-stress induced injury.

Trpm2 is expressed in the sarcolemma and transverse (t) tubules in adult mouse ventricular myocytes (Miller, Wang et al. 2013). In adult cardiac myocytes, Trpm2 is activated by H_2O_2 and intracellular ADPR, inhibited by clotrimazole and flufenamic acid, does not inactivate, and has a conductance for Ca^{2+} that is approximately 50% of that for Na^+ (Miller, Wang et al. 2013, Miller, Hoffman et al. 2014). By expressing wild-type (WT) Trpm2 or loss of function Trpm2 mutants in Trpm2-knockout (KO) cardiac myocytes, we demonstrated that Ca^{2+} influx through activated Trpm2 is required for bioenergetics maintenance and mitochondrial oxidants homeostasis (Hoffman, Miller et al. 2015). In this context, it is important to note that low levels of H_2O_2 emission which occurs during respiration in normal cardiac mitochondria (Stanley, Sivakumaran et al. 2011) may tonically activate Trpm2 channels. Physical sarcoplasmic reticulum (SR)/endoplasmic reticulum (ER)-mitochondria tethering by mitofusin-2 (de Brito and Scorrano 2008, Chen, Csordas et al. 2012) may provide the pathway by which Ca^{2+} entered via Trpm2 channels reaches the mitochondria via the SR. Constitutive, low level mitochondrial Ca^{2+} uptake is essential

in maintaining cellular bioenergetics (Cardenas, Miller et al. 2010) through stimulation of Ca^{2+}-sensitive Krebs cycle dehydrogenases (McCormack and Denton 1980), thereby increasing the availability of NADH and $FADH_2$ for the electron transport chain (Chen, Csordas et al. 2012). Because regeneration of anti-oxidative NADH is coupled to the Krebs cycle, mitochondrial Ca^{2+} uptake plays an important role in assuring efficient electron flow during oxidative phosphorylation, both for bioenergetics maintenance and to ensure that physiological but not toxic levels of ROS are generated (Kohlhaas, Liu et al. 2010).

To link Trpm2-mediated Ca^{2+} influx with cardiac bioenergetics maintenance, 4 major Ca^{2+}-dependent signaling pathways in the heart are potential candidates: Ca^{2+}-calmodulin kinase II (CaMKII), protein kinase C (PKC), calcineurin and proline-rich tyrosine kinase 2 (Pyk2). Pyk2 is a cytoplasmic enzyme activated by increased $[Ca^{2+}]_i$ resulting in autophosphorylation at Y402. In H9c2 cells, α1-adrenergic stimulation results in phosphorylation and translocation of part of pPyk2 from the cytosol to mitochondrial matrix (O-Uchi, Jhun et al. 2014). Activated Pyk2 phosphorylates mitochondrial Ca^{2+} uniporter (MCU) and promotes oligomeric MCU channel pore formation, resulting in accelerated mitochondrial Ca^{2+} uptake (O-Uchi, Jhun et al. 2014). The present study was undertaken to: (i) determine whether the H_2O_2-induced $[Ca^{2+}]_i$ increase in cardiac myocytes phosphorylates Pyk2 independent of CaMKII; (ii) evaluate whether part of phosphorylated Pyk2 translocates to the mitochondria in adult cardiac myocytes; (iii) determine whether Trpm2-mediated Pyk2 phosphorylation results in enhanced pro-survival signaling molecules in hearts subjected to ischemia/reperfusion (I/R) injury; and (iv) test whether scavenging the elevated mitochondrial oxidants in Trpm2-KO myocytes results in maintenance of mitochondrial membrane potential ($\Delta\Psi_m$). Our findings reveal that Ca^{2+} entry via Trpm2 is necessary and sufficient for Pyk2 phosphorylation. Part of Trpm2-mediated phosphorylated Pyk2 translocates to mitochondria, maintains cellular bioenergetics, reduces mitochondrial oxidants, enhances survival signaling molecules, and affords protection against I/R injury.

2. Materials and Methods

2.1 Generation of global and cardiac-specific Trpm2-KO mice and animal care.

Global and cardiac-specific Trpm2 KO mice were generated as described previously (Miller, Wang et al. 2013, Hoffman, Miller et al. 2015). At 2 mo of age, 64.0 ± 9.7% of floxed Trpm2 gene was deleted in cardiac-specific KO hearts as evaluated by qPCR and ~79% knockout rate as determined by electrophysiological measurements of cardiac Trpm2 currents (Hoffman, Miller et al. 2015). Adult mice (8 – 12 wk old) were used in this study. Mice were housed and fed on a 12:12h light-dark cycle at the Temple University Animal Facility supervised by full-time veterinarian staff members. Standard care was provided to all mice used for experiments. All protocols and procedures applied to the mice in this study were approved by the Institutional Animal Care and Use Committees of Temple University. For brevity, throughout this report, global Trpm2 KO and cardiac-specific Trpm2 KO are abbreviated as gKO and cKO, respectively, whether applied to mice, hearts or left ventricular (LV) myocytes.

2.2 Isolation of adult murine cardiac myocytes.

Cardiac myocytes were isolated from the septum and LV free wall of WT, cKO and gKO mice (8–12 wks old) according to the protocol of Zhou et al. (Zhou, Wang et al. 2000), and plated on laminin-coated glass coverslips (Tucker, Song et al. 2006) or petri dishes.

2.3 Measurement of intracellular Ca^{2+} concentration ($[Ca^{2+}]_i$) in cardiac myocytes.

Fura-2 loaded (0.67 μM fura-2 AM, Molecular Probes, Eugene, OR; 15 min, 37°C) LV myocytes attached to laminin-coated coverslips were incubated in medium 199 containing 1.8 mM extracellular Ca^{2+} concentration ($[Ca^{2+}]_o$) and 1 μM verapamil, and exposed to excitation light (360 and 380 nm) only during data acquisition. Epifluorescence (510 nm) was monitored at baseline and at 5, 10, 15 and 20 min after addition of H_2O_2 (200 μM). Daily calibration of fura-2 signals and $[Ca^{2+}]_i$ analyses were performed as previously described (Tucker, Song et al. 2006, Song, Zhang et al. 2008, Wang, Chan et al. 2009, Wang, Gao et al. 2010, Wang, Gao et al. 2011, Song, Gao et al. 2012).

2.4 Subcellular fractionation.

Cytosol and mitochondrial fractionation was performed as previously described (O-Uchi, Jhun et al. 2014). All procedures were performed at 4°C. Briefly, LV myocytes isolated from WT hearts were plated on laminin-coated culture dishes (100 mm) for 2 h. Adherent myocytes were exposed to H_2O_2 (200 μM) or phosphate buffered saline for 15 min. Myocytes were then washed with isolation buffer (IB: 320 mM sucrose, 1 mM EDTA, 10 mM Tris pH 7.4), scraped in 1ml IB per dish and centrifuged at 700g for 5 min. Cell pellets were suspended in 1 ml of IB with protease (Roche Applied Science, Indianapolis, IN) and phosphatase (Sigma-Aldrich, St. Louis, MO) inhibitor cocktails, and homogenized with Dounce homogenizer (20 strokes). Homogenate was centrifuged at 700g for 10 min. Supernatant was collected and kept on ice. Pellets were re-suspended in 0.5 ml IB with protease and phosphatase inhibitor cocktails, homogenized as before and centrifuged at 700g for 5 min. Supernatants were combined and centrifuged at 17,000g for 15 min. Supernatants were kept as cytosol, and mitochondrial pellets were suspended in 100 μl of lysis buffer and incubated overnight at 4°C with rotation.

2.5 Ischemia/Reperfusion (I/R) surgery in mice.

I/R surgery was performed as previously described (Gao, Lei et al. 2010, Miller, Wang et al. 2013, Miller, Hoffman et al. 2014). Briefly, WT, gKO and cKO mice (8–12 weeks) were anesthetized with 2% isoflurane, and the heart was exposed through a left thoracotomy at the 5^{th} intercostal space. The slipknot was tied around the left anterior descending (LAD) coronary artery 2–3 mm from its origin, and the heart was immediately returned to the chest cavity followed by evacuation of pneumothorax and closure of muscle and skin layers. The slipknot was released after 30 min. of ischemia to allow reperfusion. Sham-operated animals were subjected to the same surgical procedure except that the slipknot was not tied. Animals recovered from anesthesia within 5 min. after the completion of surgery and received ibuprofen (10 mg/50 ml drinking water) for 48 h as post-surgery analgesia. Hearts were harvested on Day 3 post-surgery. We have previously demonstrated that our I/R procedure resulted in area at risk (including both 2,3,5-triphenyltetrazolium (TTC)-negative

and TTC-positve areas but excluding Evans blue dye-positive area) that ranged from 40 to 50% of LV, and infarct sizes (TTC-negative area) ranged from 25 to 30% of area at risk in WT, gKO (Miller, Wang et al. 2013) and cKO (Hoffman, Miller et al. 2015) hearts.

2.6 Immunoblot analysis.

Heart homogenates from WT, cKO and gKO mice (both sham operated and 72h post-I/R) (Tucker, Song et al. 2006) and LV myocyte lysates (Song, Zhang et al. 2002, Song, Zhang et al. 2008) were prepared as previously described. Proteins were separated by SDS-PAGE (10, 12 or 15%) followed by transfer to Hybond-C Extra nitrocellulose (Amersham, Piscataway, NJ). Blots were blocked for 1 h with 5% milk and probed overnight with anti-pPyk2 (1:500; Invitrogen, Carlsbad, CA), anti-Pyk2 (1:250; Cell Singaling Technology Inc., Boston MA), anti-calsequestrin (1:2,000; Fitzgerald, Acton, MA), anti-pCaMKII (CaMKII phosphorylated at Thr287; 1:500; Cell Signaling Technology Inc.), anti-oCaMKII (CaMKII oxidized at Met281/282; 1:800; Genetex, Irvine, CA), anti-MCU (1:500; Dr. Madesh laboratory at Temple University), anti-GAPDH (1:2,000; Cell Signaling Technology Inc.), anti-pERK1/2 (1:1,000; Cell Signaling Technology Inc.), anti-ERK1/2 (1:2,000; Cell Signaling Technology Inc.), anti-pAkt (1:1,000; Cell Signaling Technology Inc.), or anti-Akt (1:5,000; Cell Signaling Technology Inc.) antibodies. Blots were washed and incubated with the appropriate secondary antibody conjugated to horseradish peroxidase. Enhanced chemiluminescence (Thermo Scientific, Rockford, IL) was used for the detection of signals. Intensity of the bands was quantitated with densitometry and normalized to that of calsequestrin or GAPDH (loading control).

2.7 Measurement of mitochondrial membrane potential ($\Delta\Psi_m$).

Adult WT and gKO LV myocytes were pre-incubated with the mitochondria-targeted superoxide ($O_2^{\cdot -}$) scavenger MitoTempo (50 nM, Sigma-Aldrich)(Dikalova, Bikineyeva et al. 2010, Liang, Sedlic et al. 2010) or the non-mitochondria-targeted Tempol (100 μM, VWR, Bridgeport, NJ) or vehicle for 60 min. To simulate I/R in vitro, myocytes were exposed to either 21% O_2-5% CO_2 (normoxia) or 1% O_2-5% CO_2 (hypoxia) for 30 min followed by 30 min of reoxygenation (Miller, Hoffman et al. 2014, Hoffman, Miller et al. 2015). Myocytes were incubated in Krebs-Henseleit bicarbonate (KHB) buffer (1.2 mM $[Ca^{2+}]_o$) containing 5 mM pyruvate as substrate (Cheung, Thompson et al. 1982). Following gentle centrifugation, cardiac myocytes were transferred to an intracellular-like medium (ICM) containing (in mM): KCl 120, NaCl 10, KH_2PO4 1, HEPES–Tris 20, thapsigargin (2 μg/ml), digitonin (80 μg/ml), pH 7.2; and protease inhibitors (EDTA-free complete tablets, Roche Applied Science). Permeabilized myocytes were supplemented with succinate (10 mM) and gently stirred. JC-1 (800 nM; Molecular Probes) was used to measure $\Delta\Psi_m$. Fluorescence signals were monitored in a temperature-controlled (37°C) multiwavelength-excitation and dual wavelength-emission spectrofluorometer (Delta RAM, Photon Technology International, Birmingham, NJ), using 490-nm ex/535-nm em for the monomer and 570-nm ex/595-nm em for the J-aggregate of JC-1. At 450s, 10 μM Ca^{2+} pulse was added and $\Delta\Psi_m$ (calculated as the ratio of the fluorescence of the JC-1 oligomeric to monomeric forms) was monitored. At 800s, the uncoupler carbonyl cyanide m-chlorophenyl hydrazone (CCCP; 2 μM) was added and $\Delta\Psi_m$ measured.

2.8 Confocal mitochondrial superoxide ($O_2^{\cdot -}$) measurements.

Adult WT and gKO LV myocytes were pre-incubated with MitoTempo (50 nM) or Tempol (100 μM) or vehicle for 60 min before subjected to 30 min of normoxic or hypoxic exposure followed by 30 min of reoxygenation. During reoxygenation, myocytes were loaded with the mitochondrial $O_2^{\cdot -}$ sensitive fluorophore MitoSOX Red (22 μM, Invitrogen) in extracellular media (ECM) containing 2% bovine serum albumin (BSA), 0.06% pluronic acid and 20 μM sulfinpyrazone at 37°C for 30 min. Myocytes were then washed, resuspended in ECM containing 0.25% BSA, and imaged using a Carl Zeiss Meta 510 confocal microscope (Carl Zeiss, Thornwood, NJ) with a 40x oil objective with 1.7x digital zoom at 561 nm for MitoSOX Red (Mukhopadhyay, Rajesh et al. 2007, Miller, Hoffman et al. 2014, Hoffman, Miller et al. 2015).

2.9 Statistics.

All results are expressed as means ± SE. For analysis of protein abundance as a function of group (WT vs. gKO or cKO) and treatment (e.g., H_2O_2 or I/R), two-way or three-way (group, H_2O_2 ± BAPTA) ANOVA was used. For analysis of $O_2^{\cdot -}$ levels, $[Ca^{2+}]_i$, and $\Delta\Psi_m$, one-way ANOVA was used. A commercially available software package (JMP Pro 13; SAS Institute, Cary, NC) was used. In all analyses, $p<0.05$ was taken to be statistically significant.

3. Results

3.1 Trpm2 activation by H_2O_2 phosphorylates Pyk2 and CaMKII in adult cardiac myocytes.

In adult WT LV myocytes, phosphorylation of Pyk2 was very low under basal conditions (Fig. 1). Exposure to H_2O_2 (200 μM) for 15 min resulted in ~21-fold increase in Pyk2 phosphorylation which was reduced by ~54% with the Trpm2 inhibitor clotrimazole (50 μM, 10 min) pre-treatment (Fig. 1B), suggesting Trpm2 activation resulted in Pyk2 phosphorylation. There were no changes in total Pyk2 after 15 min of H_2O_2 exposure (Fig. 1C). Activation of Trpm2 channels also resulted in phosphorylation of CaMKII (Fig. 1), which was partially blocked by clotrimazole and the CaMKII inhibitor KN93 (2 μM; 30 min pre-treatment)(Fig. 1D). Importantly, inhibiting CaMKII with KN93 did not result in statistically significant ($p=0.089$) changes in Pyk2 phosphorylation (Fig. 1B). Oxidative stress induced by H_2O_2 also resulted in oxidation of CaMKII (Fig. 1E), as expected.

3.2 Global Trpm2-KO myocytes have lower pPyk2 after H_2O_2 treatment.

Under basal conditions, phosphorylation of Pyk2 was very low in both WT and gKO myocytes (Fig. 2). Exposure to H_2O_2 resulted in ~11-fold increase in pPyk2 in WT but only ~6-fold increase in pPyk2 in gKO myocytes (Fig. 2). The differences in pPyk2 between H_2O_2–treated WT and gKO myocytes are statistically significant ($p=0.0012$, group x H_2O_2 interaction effect). These observations indicate that Pyk2 was phosphorylated by both Trpm2-dependent signaling and ROS-dependent mechanisms (Frank and Eguchi 2003). Total Pyk2 tended to be higher in gKO myocytes although the differences did not reach statistical significance ($p=0.0756$).

3.3 Tprm2-mediated $[Ca^{2+}]_i$ elevation phosphorylates Pyk2.

We have previously demonstrated that exposure to H_2O_2 (200 μM) resulted in significant increases in $[Ca^{2+}]_i$ but no changes in intracellular Na^+ concentration $(Na^+]_i)$ in WT LV myocytes, and that the $[Ca^{2+}]_i$ increase was blocked by pre-treatment with the Trpm2 inhibitor clotrimazole or by removal of extracellular Ca^{2+} (Miller, Wang et al. 2013, Hoffman, Miller et al. 2015), suggesting Trpm2-mediated Ca^{2+} influx resulted in the observed $[Ca^{2+}]_i$ elevation with H_2O_2 treatment. In the present series of experiments, H_2O_2 treatment for 20 min resulted in $[Ca^{2+}]_i$ increase by ~2.2-fold in WT myocytes (Fig. 3A). The $[Ca^{2+}]_i$ increase was completely blocked by pre-incubating the myocytes with 50 but not 10 μM of the membrane-permeable acetoxymethyl (AM) ester of the Ca^{2+} chelator 1,2-bis(o-aminophenoxy)ethane-N,N,N′,N′-tetraacetic acid (BAPTA) for 30 min (Fig. 3A). As a group, pPyk2 was higher in WT when compared to cKO myocytes (Fig. 3B & C; p=0.0034, group effect). H_2O_2 significantly increased pPyk2 ($p<0.0001$, H_2O_2 effect). BAPTA-AM pre-incubation had no detectable effect in basal Pyk2 phosphorylation but significantly reduced Pyk2 phosphorylation after H_2O_2 exposure (p=0.0032, H_2O_2 X BAPTA interaction effect). Ater H_2O_2 treatment, pPyk2 levels (with and without BAPTA-AM pre-incubation) were significantly lower in cKO when compared to WT myocytes (p=0.0068, group x H_2O_2 interaction effect). BAPTA significantly decreased pPyk2 in H_2O_2-treated WT (p=0.033) but not in H_2O_2-treated cKO (p=0.1057) myocytes. Taken together, these observations (Figs. 1, 2 and 3) strongly indicate that on activation, Trpm2-mediated Ca^{2+} influx increases $[Ca^{2+}]_i$, resulting in phosphorylation of Pyk2 in WT but not cKO myocytes. Neither H_2O_2 (p=0.6297) nor BAPTA (p=0.3753) had any effects on total Pyk2, but cKO myocytes had significantly (p=0.0020, group effect) higher total Pyk2 levels than WT myocytes (Fig. 3).

3.4 Trpm2 activation by H_2O_2 results in translocation of phosphorylated Pyk2 into mitochondria.

In H9c2 cells, α1-adrenergic stimulation promoted translocation of part of pPyk2 from the cytosol to mitochondrial matrix and accelerated mitochondrial Ca^{2+} uptake via pPyk2-dependent mitochondrial Ca^{2+} uniporter (MCU) phosphorylation and oligomeric MCU channel pore formation (O-Uchi, Jhun et al. 2014). To evaluate whether Trpm2-mediated Pyk2 phosphorylation also resulted in pPyk2 translocation into the mitochondria in adult cardiac myocytes, we first demonstrated our ability in separating total myocyte lysate into cytosolic (GADPH) and mitochondrial (MCU) fractions (Fig. 4A). In the absence of H_2O_2, pPyk2 levels were undetectably low in WT myocytes (Fig. 4B). After H_2O_2 treatment, pPyk2 levels were higher in the mitochondrial fraction when compared to cytoplasmic fraction, indicating part of pPyk2 translocated into the mitochondria (Fig. 4B).

3.5 Loss of Trpm2 results in less pPyk2 and its downstream pro-survival signaling targets after ischemia/reperfusion injury.

In the heart, both reactive oxygen species (ROS)(Tsutsui, Kinugawa et al. 2011, Miller, Wang et al. 2013, Miller, Hoffman et al. 2014, Hoffman, Miller et al. 2015) and cyclic adenosine diphosphate ribose (cADPR)(Xie, Rah et al. 2003) production are increased after I/R. Since both ROS and cADPR can activate Trpm2, we measure pPyk2 and Pyk2 in WT and cKO hearts subjected to sham operation or I/R injury. Compared to their respective

sham-operated controls, pPyk2 levels were significantly increased after I/R in both WT (p=0.015) and cKO (p=0.0125) hearts (Fig. 5A). More importantly, pPyk2 levels were significantly (p=0.0236) higher in WT-I/R when compared to cKO-I/R hearts, suggesting Trpm2 activation after I/R enhanced Pyk2 phosphorylation. There were no differences in total Pyk2 among WT-sham, WT-I/R, cKO-sham and cKO-I/R hearts. Significantly higher fractional Pyk2 phosphorylation (pPyk2/Pyk2) was also observed in gKO-I/R when compared to WT-I/R hearts (Fig. 5B). Downstream pro-survival signaling targets such as extracellular signal-regulated protein kinases 1 and 2 (ERK1/2) and protein kinase B (Akt) were less phosphorylated in gKO-I/R compared to WT-I/R hearts (Fig. 5B).

3.6 MitoTempo reduces $O_2^{\cdot -}$ levels and improves $\Delta\Psi_m$ post-H/R injury.

If Trpm2 deficiency results in less pPyk2 translocation to the mitochondria (Fig. 4) and reduced mitochondrial Ca^{2+} uptake (Miller, Hoffman et al. 2014), less efficient electron flow during oxidative phosphorylation and increased $O_2^{\cdot -}$ levels would be expected (Kohlhaas, Liu et al. 2010, Chen, Csordas et al. 2012). Although gKO myocytes tended to have higher $O_2^{\cdot -}$ levels than WT myocytes under normoxic conditions (Fig. 6, top panel), the differences did not reach statistical significance. After H/R, $O_2^{\cdot -}$ levels were much higher in gKO-H/R myocytes compared to WT-H/R myocytes ($p<0.001$), and the mitochondria-targeted $O_2^{\cdot -}$ scavenger MitoTempo reduced $O_2^{\cdot -}$ in gKO-H/R myocytes to levels not different ($p=0.760$) than those measured in WT-H/R myocytes (Fig. 6, bottom panel). The non-mitochondria-targeted ROS scavenger Tempol was also effective in reducing $O_2^{\cdot -}$ levels in gKO-H/R myocytes ($p<0.001$ compared to WT-H/R; Fig. 6, bottom panel). Effective scavenging of $O_2^{\cdot -}$ by MitoTempo in gKO-H/R myocytes was associated with improvement in mitochondrial function as indicated by restoration of $\Delta\psi_m$ (Fig. 7). In this experiment, addition of Ca^{2+} (10 μM) collapsed $\Delta\psi_m$ in gKO normoxic (Fig. 7E) but not WT normoxic (Fig. 7A) myocytes. Addition of the mitochondrial uncoupler CCCP totally collapsed $\Delta\psi_m$, as expected. After H/R, $\Delta\psi_m$ in both WT-H/R (Fig. 7B) and gKO-H/R (Fig. 7F) myocytes were low. Tempol restored $\Delta\psi_m$ in WT-H/R myocytes (Fig. 7C). Although Tempol reduced $O_2^{\cdot -}$ levels in gKO-H/R myocytes (Fig. 6), it did not restore $\Delta\psi_m$ in gKO-H/R myocytes (Fig. 7G). Only MitoTempo succeeded in reducing $O_2^{\cdot -}$ levels in gKO-H/R myocytes (Fig. 6) and in restoring $\Delta\psi_m$ in both WT-H/R (Fig. 7D) and gKO-H/R (Fig. 7H) myocytes. These observations suggest that scavenging excess $O_2^{\cdot -}$ may provide a therapeutic maneuver to protect hearts in which Trpm2 channels are inhibited.

4. Discussion

Trpm2 is expressed in many tissues including the heart, brain, hematopoietic cells and vasculature. The physiological and pathological significance of Trpm2 is just beginning to be elucidated. In organs other than the heart, Trpm2 has been implicated in bipolar disorder Type I (patients have high basal $[Ca^{2+}]_i$ in B-lymphoblasts)(Xu, Macciardi et al. 2006, Xu, Li et al. 2009), in diabetes mellitus by affecting insulin secretion mediated by increase in $[Ca^{2+}]_i$ (Herson and Ashford 1997, Uchida, Dezaki et al. 2011), and in oxidative stress-induced inhibition of autophagy and decreased cell viability mediated by Ca^{2+}-CaMKII-Beclin1 signaling pathway in mouse hepatocytes (Wang, Guo et al. 2016). In a murine model of human inflammatory bowel disease, Trpm2 -mediated Ca^{2+}

influx stimulates chemokine production in monocytes, contributing to inflammation and tissue damage (Yamamoto, Shimizu et al. 2008). These observations support the classical paradigm that increased Ca^{2+} entry with Trpm2 activation results in cytokine production, inflammation, autophagy inhibition and cell death (Sumoza-Toledo and Penner 2011, Wang, Guo et al. 2016). More recent reports, however, suggest a novel paradigm that Ca^{2+} entry via Trpm2 channels is protective in pathophysiological conditions. For example, in WT mice subjected to intraperitoneal injection of endotoxin, survival is ~5x higher than Trpm2 KO mice. This is due to Ca^{2+} entry via Trpm2 channels, thereby depolarizing plasma membrane and resulting in decreased NADPH oxidase (NOX)-mediated ROS production in WT phagocytes (Di, Gao et al. 2012). In pyramidal neurons subjected to oxidant injury, inhibition of Trpm2 results in enhanced cellular damage (Bai and Lipski 2010), confirming that Trpm2 can protect from oxidative stress. We reported that Trpm2 enhances neuroblastoma xenograft growth and reduces sensitivity to doxorubicin (Chen, Hoffman et al. 2014). Finally, a Trpm2 mutant (P1018L) was found in a subset of Guamanian amyotropic lateral sclerosis and Parkinsonism dementia patients (Hermosura, Cui et al. 2008). Unlike WT Trpm2 which does not inactivate, the P1018L mutant inactivates after channel opening by ADPR, thereby effectively limiting Ca^{2+} entry. In the heart, Trpm2 was reported to be protective against I/R injury by ameliorating mitochondrial dysfunction, maintaining cellular bioenergetics and reducing ROS levels (Miller, Wang et al. 2013, Miller, Hoffman et al. 2014, Hoffman, Miller et al. 2015) although another report suggested that Trpm2 aggravated cardiac ischemic injury by increasing neutrophil adhesion during reperfusion (Hiroi, Wajima et al. 2012). Trpm2 also ameliorated doxorubicin-induced cardiac dysfunction and prolonged survival of animals treated with doxorubicin (Hoffman, Miller et al. 2015). Finally, the recent observation that Trpm2 expression is significantly reduced in human failing hearts when compared to non-failing hearts (Morine, Paruchuri et al. 2016) provides indirect support of the hypothesis that Trpm2 is cardiac protective. Thus Ca^{2+} influx via Trpm2 channels in disease states can either be friend (decreased phagocyte NOS-mediated ROS production, maintained mitochondrial function, enhanced ATP generation and reduced mitochondrial $O_2^{\cdot -}$ levels)(Bai and Lipski 2010, Di, Gao et al. 2012, Miller, Wang et al. 2013, Chen, Hoffman et al. 2014, Miller, Hoffman et al. 2014) or foe (autophagy inhibition, Ca^{2+} overload and mitochondrial permeability transition pore (mPTP) opening, enhanced neutrophil adhesion)(Zhang, Chu et al. 2003, Yang, Chang et al. 2006, Zhang, Hirschler-Laszkiewicz et al. 2006, Yamamoto, Shimizu et al. 2008, Hiroi, Wajima et al. 2012, Wang, Guo et al. 2016), depending on the tissue, experimental model and conditions.

Recently Trpm2 was observed to be overexpressed in many tumors (Park, Chun et al. 2016) including melanoma (Orfanelli, Wenke et al. 2008), breast cancer, and neuroblastoma (Chen, Zhang et al. 2013, Chen, Hoffman et al. 2014). In some tumors, level of Trpm2 overexpression correlated with decreased patient survival (Alptekin, Eroglu et al. 2015) and increased propensity for metastasis (Li, Abuarab et al. 2016). We demonstrated that Trpm2 protected neuroblastoma cells from moderate oxidative stress, whereas cells in which Trpm2 was inhibited by the dominant-negative splice variant Trpm2-S showed increased ROS and susceptibility to cell death (Chen, Zhang et al. 2013). In vivo, growth of neuroblastoma xenografts was also inhibited by Trpm2-S (Chen, Hoffman et al. 2014). Similar to our

observations in Trpm2-KO hearts (Miller, Hoffman et al. 2014), Trpm2 inhibition in neuroblastoma resulted in increased ROS, reduced mitochondrial function, ATP production, cell viability and tumor growth, especially after doxorubicin treatment (Chen, Zhang et al. 2013, Chen, Hoffman et al. 2014). The importance of Trpm2 in promoting malignant growth and the therapeutic potential of Trpm2 inhibition are being recognized in an increasingly wide range of tumors (Miller 2012, Park, Chun et al. 2016). For example, targeting Trpm2 was recently shown to promote cell death in T cell leukemia (Klumpp, Misovic et al. 2016). Although Trpm2 inhibition can enhance the therapeutic effect of chemotherapy (e.g., doxorubicin)(Chen, Zhang et al. 2013, Chen, Hoffman et al. 2014), it may inadvertently disturb mitochondrial energy metabolism and redox balance and as such, aggravate existing ischemic heart disease (Miller, Wang et al. 2013) and doxorubicin-induced cardiomyopathy (Hoffman, Miller et al. 2015). Elucidation of mechanisms by which Trpm2 protects the heart is thus timely and will significantly contribute to the nascent field of onco-cardiology.

Trpm2 activation results in increases in $[Ca^{2+}]_i$ (Miller, Wang et al. 2013) and enhances mitochondrial Ca^{2+} uptake (Miller, Hoffman et al. 2014) in cardiac myocytes. Of the 4 major Ca^{2+} dependent signaling pathways (CaMKII, Pyk2, PKC and calcineurin) in the heart, only Pyk2 and CaMKII have been shown to directly enhance mitochondria Ca^{2+} uptake in cardiac cells (Joiner, Koval et al. 2012, O-Uchi, Jhun et al. 2014). Thus the first major finding is that Trpm2 activation phosphorylates both Pyk2 and CaMKII in the heart. In addition, inhibiting CaMKII did not significantly affect Pyk2 phosphorylation, suggesting that CaMKII had little effect on Pyk2 phosphorylation. In this study, we chose to focus on Pyk2 because: (i) Pyk2 is activated after cerebral (Tian, Litvak et al. 2000) and limb muscle (Matsui, Okigaki et al. 2007) ischemia by autophosphorylation at Y402; (ii) fractional Pyk2 phosphorylation (pPyk2/Pyk2) is increased in end-stage human non-ischemic cardiomyopathy and has been postulated to protect against arrhythmias (Lang, Glukhov et al. 2011); (iii) Ca^{2+} influx through Trpm2 activates Pyk2 and amplifies pro-survival ERK signaling in human U937 cells (Yamamoto, Shimizu et al. 2008); (iv) pPyk2 activates c-Jun N-terminal kinase (JNK) and reduces apoptosis in neonatal cardiomyocytes (Dougherty, Kubasiak et al. 2004); (v) Pyk2 is pro-survival as evidenced by its overexpression in many cancers (Lipinski and Loftus 2010); and (vi) Pyk2 inhibition decreases survival and proliferation of small cell lung cancer (Roelle, Grosse et al. 2008), breast cancer (Wendt, Schiemann et al. 2013), ovarian clear cell cancer (Yoon, Choi et al. 2014), multiple myeloma (Zhang, Moschetta et al. 2014) and prostate cancer (Hsiao, Huang et al. 2016). By contrast, published literature largely supports the concept that CaMKII activation (phosphorylation or oxidation) promotes myocyte death, cardiac hypertrophy, heart failure, and increased arrhythmogenesis (Anderson, Brown et al. 2011, Joiner, Koval et al. 2012, Luczak and Anderson 2014, Anderson 2015, Mattiazzi, Bassani et al. 2015).

The second major finding is that H_2O_2 treatment resulted in significantly less Pyk2 phosphorylation in both gKO (~40%) and cKO (~50%) myocytes when compared to WT myocytes, confirming the important role of Trpm2 in Pyk2 activation. In addition, buffering Trpm2-mediated $[Ca^{2+}]_i$ increase by BAPTA significantly reduced Pyk2 phosphorylation in WT but not cKO myocytes. These two observations indicate that Ca^{2+} influx via activated Trpm2 channels mediated Pyk2 phosphorylation. An unexpected finding is that total Pyk2 tended to be higher in gKO and significantly higher in cKO compared to their respective

WT controls. This suggests that after exposure to H_2O_2, the fractional Pyk2 phosphorylation is lower in KO compared to WT myocytes. Indeed, fractional Pyk2 phosphorylation was ~5-fold lower in cKO when compared to WT myocytes exposed to H_2O_2 ($p=0.0036$, group x H_2O_2 interaction effect).

Following phosphorylation, part of pPyk2 translocated to the mitochondria and enhanced mitochondrial Ca^{2+} uptake (Miller, Hoffman et al. 2014). We hypothesized the mechanism is similar to what we reported for H9c2 cardiomyocytes after α-adrenergic stimulation (O-Uchi, Jhun et al. 2014). Maintenance of physiological mitochondrial Ca^{2+} uptake is indispensable in cellular bioenergetics (Cardenas, Miller et al. 2010) and mitochondrial oxidant homeostasis (Kohlhaas, Liu et al. 2010).

The third major finding is that Pyk2 activation was much less robust in cKO compared to WT hearts after I/R injury. Similarly, post-I/R, fractional Pyk2 phosphorylation was much less in gKO compared to WT hearts. Downstream pro-survival signaling targets such as ERK1/2 and Akt were less phosphorylated in gKO-I/R compared to WT-I/R hearts. Our results in the heart are in agreement with those observed in human U937 cells, in which Trpm2-mediated Ca^{2+} influx phosphorylates Pyk2 and amplifies pro-survival signaling ERK pathways (Yamamoto, Shimizu et al. 2008). These results suggest that Trpm2 may protect against oxidative injury not only by maintenance of cellular bioenergetics and reducing toxic levels of oxidants, but also by activating pro-survival signaling pathways in the heart.

We have previously demonstrated that Trpm2 deficiency resulted in reduced levels of Complex I [NADH dehydrogenase (ubiquinone) 1α subcomplex 4-like 2 (NDUFA4L2)] (Miller, Hoffman et al. 2014, Hoffman, Miller et al. 2015) and Complex IV (Miller, Hoffman et al. 2014) in cardiac mitochondria, especially after ischemia/reperfusion. We have also shown by patch-clamp that the intrinsic MCU activity was significantly lower in gKO mitoplasts (Miller, Hoffman et al. 2014). Decreased levels of respiratory electron transport complexes and reduced intrinsic MCU activity due to less pPyk2 translocation to the mitochondria are two independent mechanisms that conspired together to reduce mitochondrial Ca^{2+} uptake and electron transport activity to account for the observed lower oxygen consumption rate and mitochondrial membrane potential, reduced ATP levels, and elevated ROS levels in Trpm2 deficient hearts (Miller, Hoffman et al. 2014, Hoffman, Miller et al. 2015).

Since Trpm2 facilitates mitochondrial Ca^{2+} uptake in the heart (Miller, Hoffman et al. 2014), one major consequence of Trpm2 deficiency or inhibition would be inefficient electron flow during oxidative phosphorylation, resulting in increased ROS levels. This is what we previously reported (Miller, Hoffman et al. 2014, Hoffman, Miller et al. 2015). From a therapeutic standpoint, it would be useful to test if ROS scavengers could alleviate some of the mitochondrial dysfunction brought on by Trpm2 deficiency or inhibition, under both basal and post-I/R conditions. Thus the final major finding is that the mitochondria-targeted $O_2^{\cdot -}$ scavenger MitoTempo, but not the cytoplasmic ROS scavenger Tempol, reduced $O_2^{\cdot -}$ levels and restored $\Delta\Psi_m$ towards normal in gKO myocytes after hypoxia/reoxygenation. This observation suggests that mitochondrial $O_2^{\cdot -}$ is the major ROS species affected by Trmp2 deficiency or inhibition, and that mitochondria-targeted $O_2^{\cdot -}$ scavengers (MitoTempo

and oral MitoQ)(Mercer, Yu et al. 2012) may be useful in protecting hearts from therapeutic Trpm2 inhibition in cancer patients (Miller 2012).

In summary, Trpm2-mediated Ca^{2+} influx regulated mitochondrial Ca^{2+} uptake in the heart by Pyk2 phosphorylation followed by its translocation to the mitochondria resulting in enhanced mitochondrial Ca^{2+} uptake (Fig. 8). Trpm2-mediated Pyk2 activation protected the heart from oxidative injury not only by assuring efficient electron flow during oxidative phosphorylation and thereby maintaining cellular bioenergetics and minimizing toxic levels of mitochondrial superoxide, but also by activating downstream pro-survival signaling pathways such as Akt and ERK1/2 (Fig. 8). Finally, mitochondria-targeted superoxide scavengers might have a beneficial role in protecting the heart from therapeutic Trpm2 inhibition.

Acknowledgments

This work was supported in part by National Institutes of Health Grants RO1-DK46778 and R01-GM117014 (BAM); RO1-HL86699 (MM); PO1-HL91799 (Project 2) and RO1-HL123093 (AMF); RO1-HL137426, RO1-HL123093, UO1-NS097162 and R21-NS098991 (JYC); and RO1-HL093671, RO1-HL122124 and RO1-HL137266 (SSS).

8. References

Alptekin M, Eroglu S, Tutar E, Sencan S, Geyik MA, Ulasli M, Demiryurek AT and Camci C (2015). “Gene expressions of TRP channels in glioblastoma multiforme and relation with survival.” Tumour Biol 36(12): 9209–9213. [PubMed: 26088448]

Anderson ME (2015). “Oxidant stress promotes disease by activating CaMKII.”.” J Mol Cell Cardiol 89(Pt B): 160–167. [PubMed: 26475411]

Anderson ME, Brown JH and Bers DM (2011). “CaMKII in myocardial hypertrophy and heart failure.” J Mol Cell Cardiol 51(4): 468–473. [PubMed: 21276796]

Bai JZ and Lipski J (2010). “Differential expression of TRPM2 and TRPV4 channels and their potential role in oxidative stress-induced cell death in organotypic hippocampal culture.” Neurotoxicology 31(2): 204–214. [PubMed: 20064552]

Cardenas C, Miller RA, Smith I, Bui T, Molgo J, Muller M, Vais H, Cheung KH, Yang J, Parker I, Thompson CB, Birnbaum MJ, Hallows KR and Foskett JK (2010). “Essential regulation of cell bioenergetics by constitutive InsP3 receptor Ca^{2+} transfer to mitochondria.” Cell 142(2): 270–283. [PubMed: 20655468]

Chen SJ, Hoffman NE, Shanmughapriya S, Bao L, Keefer K, Conrad K, Merali S, Takahashi Y, Abraham T, Hirschler-Laszkiewicz I, Wang J, Zhang XQ, Song J, Barrero Y. C, Shi Y, Kawasawa I, Bayerl M, Sun T, Barbour M, Wang HG, Madesh M, Cheung JY and Miller BA (2014). “A splice variant of the human ion channel TRPM2 modulates neuroblastoma tumor growth through hypoxia-inducible factor (HIF)-1/2α.” J Biol Chem.289(52): 36284–36302. [PubMed: 25391657]

Chen SJ, Zhang W, Tong Q, Conrad K, Hirschler-Laszkiewicz I, Bayerl M, Kim JK, Cheung JY and Miller BA (2013). “Role of TRPM2 in cell proliferation and susceptibility to oxidative stress.” Am J Physiol Cell Physiol 304(6): C548–560. [PubMed: 23302782]

Chen Y, Csordas G, Jowdy C, Schneider TG, Csordas N, Wang W, Liu Y, Kohlhaas M, Meiser M, Bergem S, Nerbonne JM, Dorn GW 2nd and Maack C (2012). “Mitofusin 2-containing mitochondrial-reticular microdomains direct rapid cardiomyocyte bioenergetic responses via interorganelle Ca^{2+} crosstalk.” Circ Res 111(7): 863–875. [PubMed: 22777004]

Cheung JY, Thompson IG and Bonventre JV (1982). “Effects of extracellular calcium removal and anoxia on isolated rat myocytes.” Am J Physiol Cell Physiology 243: C184–C190.

de Brito OM and Scorrano L (2008). “Mitofusin 2 tethers endoplasmic reticulum to mitochondria.”.” Nature 456(7222): 605–610. [PubMed: 19052620]

Di A, Gao XP, Qian F, Kawamura T, Han J, Hecquet C, Ye RD, Vogel SM and Malik AB (2012). "The redox-sensitive cation channel TRPM2 modulates phagocyte ROS production and inflammation." Nat Immunol 13(1): 29–34.

Dikalova AE, Bikineyeva AT, Budzyn K, Nazarewicz RR, McCann L, Lewis W, Harrison DG and Dikalov SI (2010). "Therapeutic targeting of mitochondrial superoxide in hypertension." Circ Res 107(1): 106–116. [PubMed: 20448215]

Dougherty CJ, Kubasiak LA, Frazier DP, Li H, Xiong WC, Bishopric NH and Webster KA (2004). "Mitochondrial signals initiate the activation of c-Jun N-terminal kinase (JNK) by hypoxia-reoxygenation." FASEB J 18(10): 1060–1070. [PubMed: 15226266]

Frank GD and Eguchi S (2003). "Activation of tyrosine kinases by reactive oxygen species in vascular smooth muscle cells: significance and involvement of EGF receptor transactivation by angiotensin II." Antioxid Redox Signal 5(6): 771–780. [PubMed: 14588150]

Gao E, Lei YH, Shang X, Huang ZM, Zuo L, Boucher M, Fan Q, Chuprun JK, Ma XL and Koch WJ (2010). "A novel and efficient model of coronary artery ligation and myocardial infarction in the mouse." Circ Res 107(12): 1445–1453. [PubMed: 20966393]

Hara Y, Wakamori M, Ishii M, Maeno E, Nishida M, Yoshida T, Yamada H, Shimizu S, Mori E, Kudoh J, Shimizu N, Kurose H, Okada Y, Imoto K and Mori Y (2002). "LTRPC2 Ca^{2+}-permeable channel activated by changes in redox status confers susceptibility to cell death." Mol Cell 9(1): 163–173. [PubMed: 11804595]

Hecquet CM, Ahmmed GU, Vogel SM and Malik AB (2008). "Role of TRPM2 channel in mediating H_2O_2-induced Ca^{2+} entry and endothelial hyperpermeability." Circ Res 102(3): 347–355. [PubMed: 18048770]

Hermosura MC, Cui AM, Go RC, Davenport B, Shetler CM, Heizer JW, Schmitz C, Mocz G, Garruto RM and Perraud AL (2008). "Altered functional properties of a TRPM2 variant in Guamanian ALS and PD." Proc Natl Acad Sci U S A 105(46): 18029–18034. [PubMed: 19004782]

Herson PS and Ashford ML (1997). "Activation of a novel non-selective cation channel by alloxan and H_2O_2 in the rat insulin-secreting cell line CRI-G1." J Physiol 501 (Pt 1): 59–66. [PubMed: 9174994]

Hiroi T, Wajima T, Negoro T, Ishii M, Nakano Y, Kiuchi Y, Mori Y and Shimizu S (2012). "Neutrophil TRPM2 channels are implicated in the exacerbation of myocardial ischemia/reperfusion injury." Cardiovasc Res 97: 271–281. [PubMed: 23129587]

Hoffman NE, Miller BA, Wang J, Elrod JW, Rajan S, Gao E, Song J, Zhang XQ, Hirschler-Laszkiewicz I, Shanmughapriya S, Koch WJ, Feldman AM, Madesh M and Cheung JY (2015). "Ca^{2+} entry via Trpm2 is essential for cardiac myocyte bioenergetics maintenance." Am J Physiol Heart Circ Physiol 308(6): H637–650. [PubMed: 25576627]

Hsiao YH, Huang YT, Hung CY, Kuo TC, Luo FJ and Yuan TC (2016). "PYK2 via S6K1 regulates the function of androgen receptors and the growth of prostate cancer cells." Endocr Relat Cancer 23(8): 651–663. [PubMed: 27492635]

Joiner ML, Koval OM, Li J, He BJ, Allamargot C, Gao Z, Luczak ED, Hall DD, Fink BD, Chen B, Yang J, Moore SA, Scholz TD, Strack S, Mohler PJ, Sivitz WI, Song LS and Anderson ME (2012). "CaMKII determines mitochondrial stress responses in heart." Nature 491(7423): 269–273. [PubMed: 23051746]

Klumpp D, Misovic M, Szteyn K, Shumilina E, Rudner J and Huber SM (2016). "Targeting TRPM2 channels impairs radiation-induced cell cycle arrest and fosters cell death of T cell leukemia cells in a Bcl-2-dependent manner." Oxid Med Cell Longev 2016: 8026702. [PubMed: 26839633]

Kohlhaas M, Liu T, Knopp A, Zeller T, Ong MF, Bohm M, O'Rourke B and Maack C (2010). "Elevated cytosolic Na^+ increases mitochondrial formation of reactive oxygen species in failing cardiac myocytes." Circulation 121(14): 1606–1613. [PubMed: 20351235]

Lang D, Glukhov AV, Efimova T and Efimov IR (2011). "Role of Pyk2 in cardiac arrhythmogenesis." Am J Physiol Heart Circ Physiol 301(3): H975–983. [PubMed: 21666110]

Li F, Abuarab N and Sivaprasadarao A (2016). "Reciprocal regulation of actin cytoskeleton remodelling and cell migration by Ca^{2+} and Zn^{2+}: role of TRPM2 channels." J Cell Sci 129(10): 2016–2029. [PubMed: 27068538]

Liang HL, Sedlic F, Bosnjak Z and Nilakantan V (2010). "SOD1 and MitoTEMPO partially prevent mitochondrial permeability transition pore opening, necrosis, and mitochondrial apoptosis after ATP depletion recovery." Free Radic Biol Med 49(10): 1550–1560. [PubMed: 20736062]

Lipinski CA and Loftus JC (2010). "Targeting Pyk2 for therapeutic intervention." Expert Opin Ther Targets 14(1): 95–108. [PubMed: 20001213]

Luczak ED and Anderson ME (2014). "CaMKII oxidative activation and the pathogenesis of cardiac disease." J Mol Cell Cardiol 73: 112–116. [PubMed: 24530899]

Matsui A, Okigaki M, Amano K, Adachi Y, Jin D, Takai S, Yamashita T, Kawashima S, Kurihara T, Miyazaki M, Tateishi K, Matsunaga S, Katsume A, Honshou S, Takahashi T, Matoba S, Kusaba T, Tatsumi T and Matsubara H (2007). "Central role of calcium-dependent tyrosine kinase PYK2 in endothelial nitric oxide synthase-mediated angiogenic response and vascular function." Circulation 116(9): 1041–1051. [PubMed: 17698736]

Mattiazzi A, Bassani RA, Escobar AL, Palomeque J, Valverde CA, Vila Petroff M and Bers DM (2015). "Chasing cardiac physiology and pathology down the CaMKII cascade." Am J Physiol Heart Circ Physiol 308(10): H1177–1191. [PubMed: 25747749]

McCormack JG and Denton RM (1980). "Role of calcium ions in the regulation of intramitochondrial metabolism. Properties of the Ca^{2+}-sensitive dehydrogenases within intact uncoupled mitochondria from the white and brown adipose tissue of the rat." Biochem J 190(1): 95–105. [PubMed: 6778477]

Mercer JR, Yu E, Figg N, Cheng KK, Prime TA, Griffin JL, Masoodi M, VidalPuig A, Murphy MP and Bennett MR (2012). "The mitochondria-targeted antioxidant MitoQ decreases features of the metabolic syndrome in $ATM^{+/-}$/$ApoE^{-/-}$ mice." Free Radic Biol Med 52(5): 841–849. [PubMed: 22210379]

Miller BA (2012). "TRPM2 function and potential as a drug target." Methods in Pharmacol Toxicol I(TRP Channels in Drug Discovery): 89–102.

Miller BA, Hoffman NE, Merali S, Zhang XQ, Wang J, Rajan S, Shanmughapriya S, Gao E, Barrero CA, Mallilankaraman K, Song J, Gu T, Hirschler-Laszkiewicz I, Koch WJ, Feldman AM, Madesh M and Cheung JY (2014). "TRPM2 channels protect against cardiac ischemia-reperfusion injury: role of mitochondria." J Biol Chem 289(11): 7615–7629. [PubMed: 24492610]

Miller BA, Wang J, Hirschler-Laszkiewicz I, Gao E, Song J, Zhang XQ, Koch WJ, Madesh M, Mallilankaraman K, Gu T, Chen SJ, Keefer K, Conrad K, Feldman AM and Cheung JY (2013). "The second member of transient receptor potential-melastatin channel family protects hearts from ischemia-reperfusion injury." Am J Physiol Heart Circ Physiol 304(7): H1010–1022. [PubMed: 23376831]

Miller BA and Zhang W (2011). "TRP channels as mediators of oxidative stress." Adv Exp Med Biol 704: 531–544. [PubMed: 21290315]

Morine KJ, Paruchuri V, Qiao X, Aronovitz M, Huggins GS, DeNofrio D, Kiernan MS, Karas RH and Kapur NK (2016). "Endoglin selectively modulates transient receptor potential channel expression in left and right heart failure." Cardiovasc Pathol 25(6): 478–482. [PubMed: 27614169]

Mukhopadhyay P, Rajesh M, Hasko G, Hawkins BJ, Madesh M and Pacher P (2007). "Simultaneous detection of apoptosis and mitochondrial superoxide production in live cells by flow cytometry and confocal microscopy." Nat Protoc 2(9): 2295–2301. [PubMed: 17853886]

Nilius B, Owsianik G, Voets T and Peters JA (2007). "Transient receptor potential cation channels in disease." Physiol Rev 87(1): 165–217. [PubMed: 17237345]

O-Uchi J, Jhun BS, Xu S, Hurst S, Raffaello A, Liu X, Yi B, Zhang H, Gross P, Mishra J, Ainbinder A, Kettlewell S, Smith GL, Dirksen RT, Wang W, Rizzuto R and Sheu SS (2014). "Adrenergic signaling regulates mitochondrial Ca^{2+} uptake through Pyk2-dependent tyrosine phosphorylation of the mitochondrial Ca^{2+} uniporter." Antioxid Redox Signal 21(6): 863–879. [PubMed: 24800979]

Orfanelli U, Wenke AK, Doglioni C, Russo V, Bosserhoff AK and Lavorgna G (2008). "Identification of novel sense and antisense transcription at the TRPM2 locus in cancer." Cell Res 18(11): 1128–1140. [PubMed: 18957938]

Park YR, Chun JN, So I, Kim HJ, Baek S, Jeon JH and Shin SY (2016). "Datadriven analysis of TRP channels in cancer: Linking variation in gene expression to clinical significance." Cancer Genomics Proteomics 13(1): 83–90. [PubMed: 26708603]

Roelle S, Grosse R, Buech T, Chubanov V and Gudermann T (2008). "Essential role of Pyk2 and Src kinase activation in neuropeptide-induced proliferation of small cell lung cancer cells." Oncogene 27(12): 1737–1748. [PubMed: 17906699]

Sano Y, Inamura K, Miyake A, Mochizuki S, Yokoi H, Matsushime H and Furuichi K (2001). "Immunocyte Ca^{2+} influx system mediated by LTRPC2." Science 293(5533): 1327–1330. [PubMed: 11509734]

Song J, Gao E, Wang J, Zhang XQ, Chan TO, Koch WJ, Shang X, Joseph JI, Peterson BZ, Feldman AM and Cheung JY (2012). "Constitutive overexpression of phospholemman S68E mutant results in arrhythmias, early mortality and heart failure: Potenial involvement of Na^+/Ca^{2+} exchanger." Am J Physiol Heart Circ Physiol 302: H770–H781. [PubMed: 22081699]

Song J, Zhang XQ, Carl LL, Qureshi A, Rothblum LI and Cheung JY (2002). "Overexpression of phospholemman alter contractility and $[Ca^{2+}]_i$ transients in adult rat myocytes." Am. Journal of Physiol. Heart Circ. Physiol. 283: H576–H583. [PubMed: 12124204]

Song J, Zhang XQ, Wang J, Cheskis E, Chan TO, Feldman AM, Tucker AL and Cheung JY (2008). "Regulation of cardiac myocyte contractility by phospholemman:Na^+/Ca^{2+} exchange vs. Na^+-K^+-ATPase." Am J Physiol Heart Circ Physiol 295: H1615–H1625. [PubMed: 18708446]

Stanley BA, Sivakumaran V, Shi S, McDonald I, Lloyd D, Watson WH, Aon MA and Paolocci N (2011). "Thioredoxin reductase-2 is essential for keeping low levels of H_2O_2 emission from isolated heart mitochondria." J Biol Chem 286(38): 33669–33677. [PubMed: 21832082]

Sumoza-Toledo A and Penner R (2011). "TRPM2: a multifunctional ion channel for calcium signalling." J Physiol 589(Pt 7): 1515–1525. [PubMed: 21135052]

Takahashi N, Kozai D, Kobayashi R, Ebert M and Mori Y (2011). "Roles of TRPM2 in oxidative stress."Cell Calcium 50(3): 279–287. [PubMed: 21616534]

Tian D, Litvak V and Lev S (2000). "Cerebral ischemia and seizures induce tyrosine phosphorylation of PYK2 in neurons and microglial cells." J Neurosci 20(17): 6478–6487. [PubMed: 10964954]

Tsutsui, Kinugawa S and Matsushima S (2011). "Oxidative stress and heart failure." Am J Physiol Heart Circ Physiol 301(6): H2181–2190. [PubMed: 21949114]

Tucker AL, Song J, Zhang XQ, Wang J, Ahlers BA, Carl LL, Mounsey JP, Moorman JR, Rothblum LI and Cheung JY (2006). "Altered contractility and $[Ca^{2+}]_i$ homeostasis in phospholemman-deficient murine myocytes: Role of Na^+/Ca^{2+} exchange." Am J Physiol Heart Circ Physiol 291: H2199–H2209. [PubMed: 16751288]

Uchida K, Dezaki K, Damdindorj B, Inada H, Shiuchi T, Mori Y, Yada T, Minokoshi Y and Tominaga M (2011). "Lack of TRPM2 impaired insulin secretion and glucose metabolisms in mice." Diabetes 60(1): 119–126. [PubMed: 20921208]

Wang J, Chan TO, Zhang XQ, Gao E, Song J, Koch WJ, Feldman AM and Cheung JY (2009). "Induced overexpression of Na^+/Ca^{2+} exchanger transgene: Altered myocyte contractility, $[Ca^{2+}]_i$ transients, SR Ca^{2+} contents and action potential duration." Am J Physiol Heart Circ Physiol 297: H590–H601. [PubMed: 19525383]

Wang J, Gao E, Rabinowitz J, Song J, Zhang XQ, Koch WJ, Tucker AL, Chan TO, Feldman AM and Cheung JY (2011). "Regulation of in vivo cardiac contractility by phospholemman: role of Na^+/Ca^{2+} exchange." Am J Physiol Heart Circ Physiol 300(3): H859–868. [PubMed: 21193587]

Wang J, Gao E, Song J, Zhang XQ, Li J, Koch WJ, Tucker AL, Philipson KD, Chan TO, Feldman AM and Cheung JY (2010). "Phospholemman and β-adrenergic stimulation in the heart." Am J Physiol Heart Circ Physiol 298(3): H807–815. [PubMed: 20008271]

Wang Q, Guo W, Hao B, Shi X, Lu Y, Wong CW, Ma VW, Yip TT, Au JS, Hao Q, Cheung KH, Wu W, Li GR and Yue J (2016). "Mechanistic study of TRPM2-Ca^{2+}-CAMK2-BECN1 signaling in oxidative stress-induced autophagy inhibition." Autophagy 12(8): 1340–1354. [PubMed: 27245989]

Wendt MK, Schiemann BJ, Parvani JG, Lee YH, Kang Y and Schiemann WP (2013). "TGF-β stimulates Pyk2 expression as part of an epithelial-mesenchymal transition program required for metastatic outgrowth of breast cancer." Oncogene 32(16): 2005–2015. [PubMed: 22710711]

Xie GH, Rah SY, Yi KS, Han MK, Chae SW, Im MJ and Kim UH (2003). “Increase of intracellular Ca^{2+} during ischemia/reperfusion injury of heart is mediated by cyclic ADP-ribose.” Biochem Biophys Res Commun 307(3): 713–718. [PubMed: 12893282]

Xu C, Li PP, Cooke RG, Parikh SV, Wang K, Kennedy JL and Warsh JJ (2009). “TRPM2 variants and bipolar disorder risk: confirmation in a family-based association study.” Bipolar Disord 11(1): 1–10.

Xu C, Macciardi F, Li PP, Yoon IS, Cooke RG, Hughes B, Parikh SV, McIntyre RS, Kennedy JL and Warsh JJ (2006). “Association of the putative susceptibility gene, transient receptor potential protein melastatin type 2, with bipolar disorder.” Am J Med Genet B Neuropsychiatr Genet 141B(1): 36–43. [PubMed: 16252251]

Yamamoto S, Shimizu S, Kiyonaka S, Takahashi N, Wajima T, Hara Y, Negoro T, Hiroi T, Kiuchi Y, Okada T, Kaneko S, Lange I, Fleig A, Penner R, Nishi M, Takeshima H and Mori Y (2008). “TRPM2-mediated Ca^{2+}influx induces chemokine production in monocytes that aggravates inflammatory neutrophil infiltration.” Nat Med 14(7): 738–747. [PubMed: 18542050]

Yang KT, Chang WL, Yang PC, Chien CL, Lai MS, Su MJ and Wu ML (2006). “Activation of the transient receptor potential M2 channel and poly(ADP-ribose) polymerase is involved in oxidative stress-induced cardiomyocyte death.”Cell Death Differ 13(10): 1815–1826. [PubMed: 16294211]

Yoon H, Choi YL, Song JY, Do I, Kang SY, Ko YH, Song S and Kim BG (2014). “Targeted inhibition of FAK, PYK2 and BCL-XL synergistically enhances apoptosis in ovarian clear cell carcinoma cell lines.” PLoS One 9(2): e88587. [PubMed: 24523919]

Zhang W, Chu X, Tong Q, Cheung JY, Conrad K, Masker K and Miller BA (2003). “A novel TRPM2 isoform inhibits calcium influx and susceptibility to cell death.” J Biol Chem 278: 16222–16229. [PubMed: 12594222]

Zhang W, Hirschler-Laszkiewicz I, Tong Q, Conrad K, Sun SC, Penn L, Barber DL, Stahl R, Carey DJ, Cheung JY and Miller BA (2006). “TRPM2 is an ion channel that modulates hematopoietic cell death through activation of caspases and PARP cleavage.” Am J Physiol Cell Physiol 290(4): C1146–1159. [PubMed: 16306129]

Zhang Y, Moschetta M, Huynh D, Tai YT, Zhang Y, Zhang W, Mishima Y, Ring JE, Tam WF, Xu Q, Maiso P, Reagan M, Sahin I, Sacco A, Manier S, Aljawai Y, Glavey S, Munshi NC, Anderson KC, Pachter J, Roccaro AM and Ghobrial IM (2014). “Pyk2 promotes tumor progression in multiple myeloma.” Blood 124(17): 2675–2686. [PubMed: 25217697]

Zhou YY, Wang SQ, Zhu WZ, Chruscinski A, Kobilka BK, Ziman B, Wang S, Lakatta EG, Cheng H and Xiao RP (2000). “Culture and adenoviral infection of adult mouse cardiac myocytes: methods for cellular genetic physiology.” Am J Physiol Heart Circ Physiol 279(1): H429–436. [PubMed: 10899083]

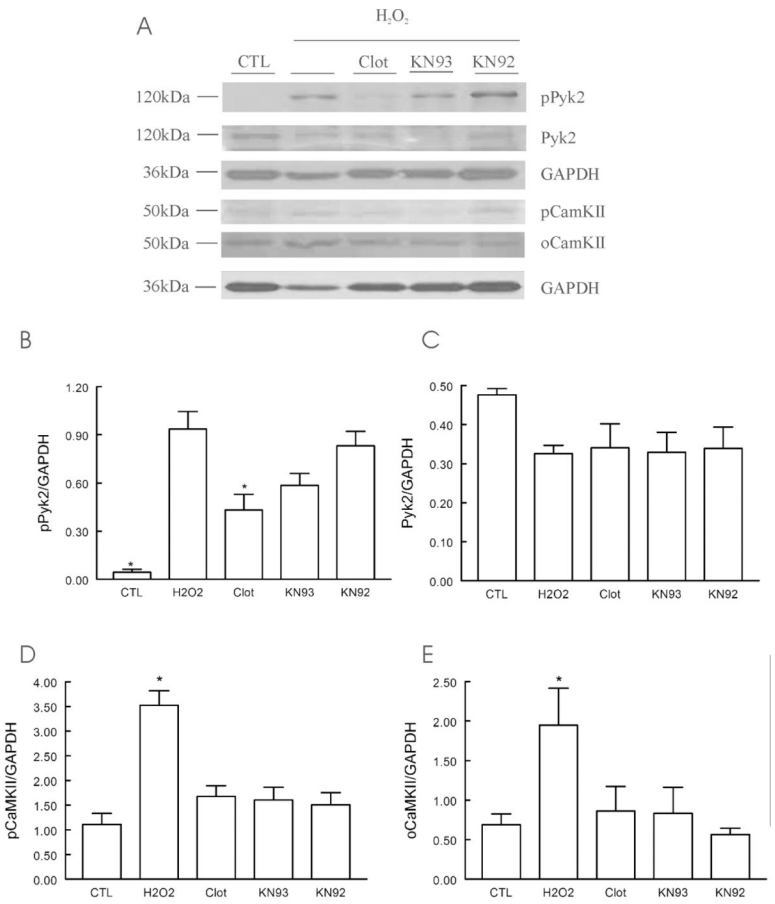

Figure 1. Trpm2 activation results in Pyk2 and CaMKII phosphorylation.

LV myocytes isolated from WT hearts were incubated in Media 199 (containing 1 μM verapamil) and exposed to vehicle (CTL) or 200 μM H_2O_2 for 15 min before harvest for immunoblotting. In some experiments, myocytes were pre-incubated with Trpm2 inhibitor clotrimazole (Clot; 50 μM, 10 min), the CaMKII inhibitor KN93 (2 μM, 30 min) or its inactive control KN92 (2 μM, 30 min) before H_2O_2 exposure. A: representative blot of an experiment. B: summary of pPyk2/GAPDH of 5 separate myocyte preparations. *$p<0.004$, H_2O_2 vs.clotrimazole or CTL. C: summary of total Pyk2/GAPDH of 3 myocyte preparations. D: summary of pCaMKII (phosphorylated at Thr287) of 3 myocyte preparations. *$p<0.02$, H_2O_2 vs. CTL or clotrimazole or KN93 or KN92. D: summary of oCaMKII (oxidized at Met281/282) of 3 myocyte preparations. *$p<0.05$, H_2O_2 vs. CTL or KN92.

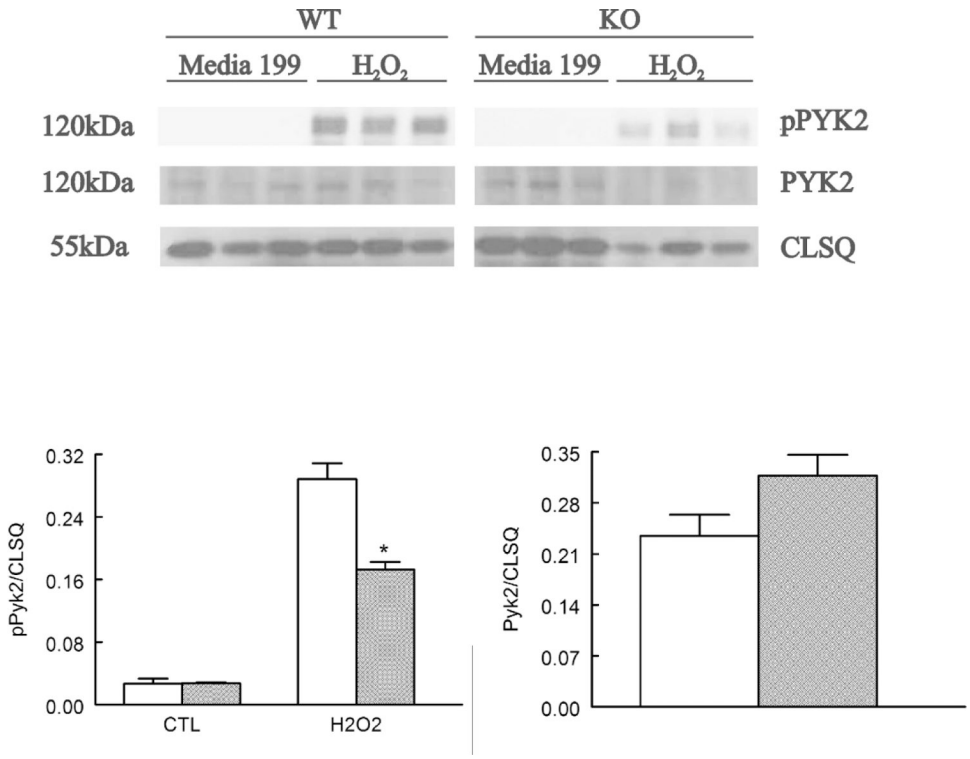

Figure 2. H_2O_2 exposure results in less Pyk2 phosphorylation in global Trpm2 KO myocytes.

LV myocytes isolated from WT and gKO hearts were incubated in Media 199 (containing 1 μM verapamil) and exposed to vehicle (Media 199) or 200 μM H_2O_2 for 15 min before harvesting for immunoblotting. Top: Western blots of pPyk2 and Pyk2. Calsequestrin (CLSQ) was used as a loading control. Bottom: summary of pPyK2/CLSQ for 3 WT (open bars) and 3 gKO (gray bars) myocyte preparations. Two-way ANOVA showed significant group ($p=0.0012$), H_2O_2 ($p<0.0001$) and group x H_2O_2 interaction (*$p=0.0012$) effects. Total Pyk2/CLSQ tended to be higher in gKO myocytes although the difference did not reach statistical significance ($p=0.0756$).

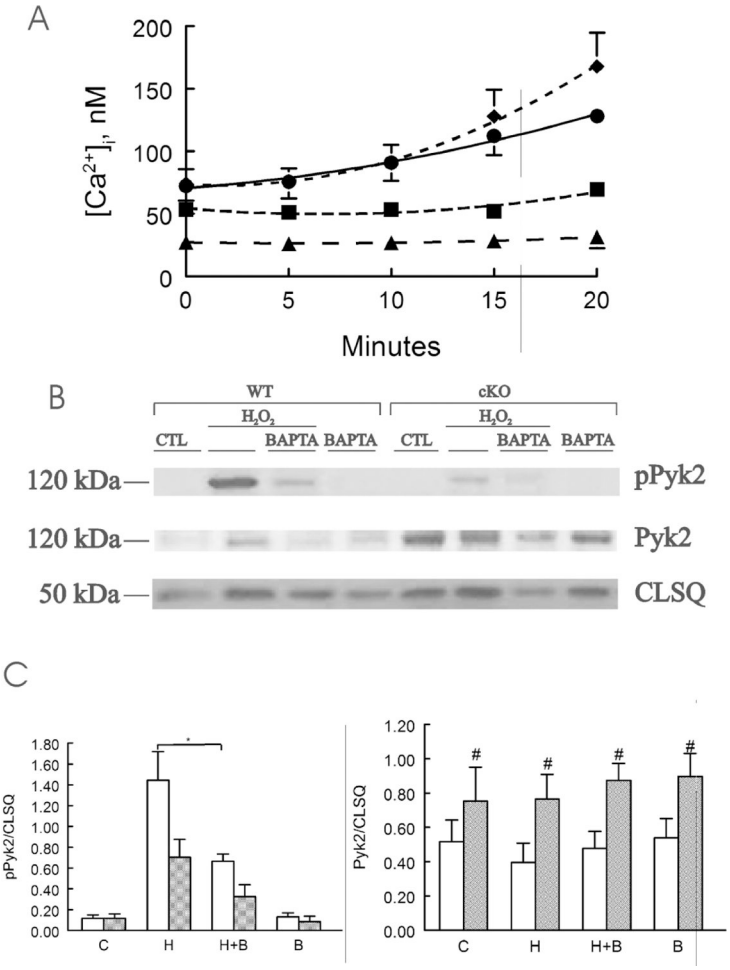

Figure 3. BAPTA buffers H_2O_2 induced $[Ca^{2+}]_i$ increase and reduces Pyk2 phosphorylation in WT but not in cardiac-specific Trpm2 KO myocytes.

A. LV myocytes isolated from WT hearts were loaded with the Ca^{2+} indicator fura2 (0.67 μM fura-2 AM, 15 min, 37°C) before exposure to vehicle (■, n=4) or H_2O_2 (200 μM; ♦, n=4) and $[Ca^{2+}]_i$ followed for 20 min. Some myocytes were pre-incubated with either 10 (•. n=4) or 50 μM (▲, n=4) of BAPTA-AM for 30 min before H_2O_2. B. LV myocytes isolated from WT and cKO hearts were treated with vehicle (CTL) or H_2O_2 (200 μM) for 15 min, with or without pre-incubation with BAPTA-AM (50 μM, 30 min), before harvest for immunoblotting. Representative blot of pPyk2, Pyk2 and calsequestrin (CLSQ; loading control) of 1 of 5 separate myocyte preparations. C. Summary of pPyk2/CLSQ and Pyk2/CLSQ for 4 WT (open bars) and 5 cKO (gray bars) myocyte preparations under control (C), H_2O_2 (H), H_2O_2 + BAPTA (H + B) and BAPTA (B) conditions. BAPTA significantly decreased pPyk2/CLSQ in WT (*, p=0.033) but not in cKO (p=0.1057) myocytes after H_2O_2 treatment. Total Pyk2/CLSQ in cKO was significantly higher (#, p=0.0020) than WT myocytes.

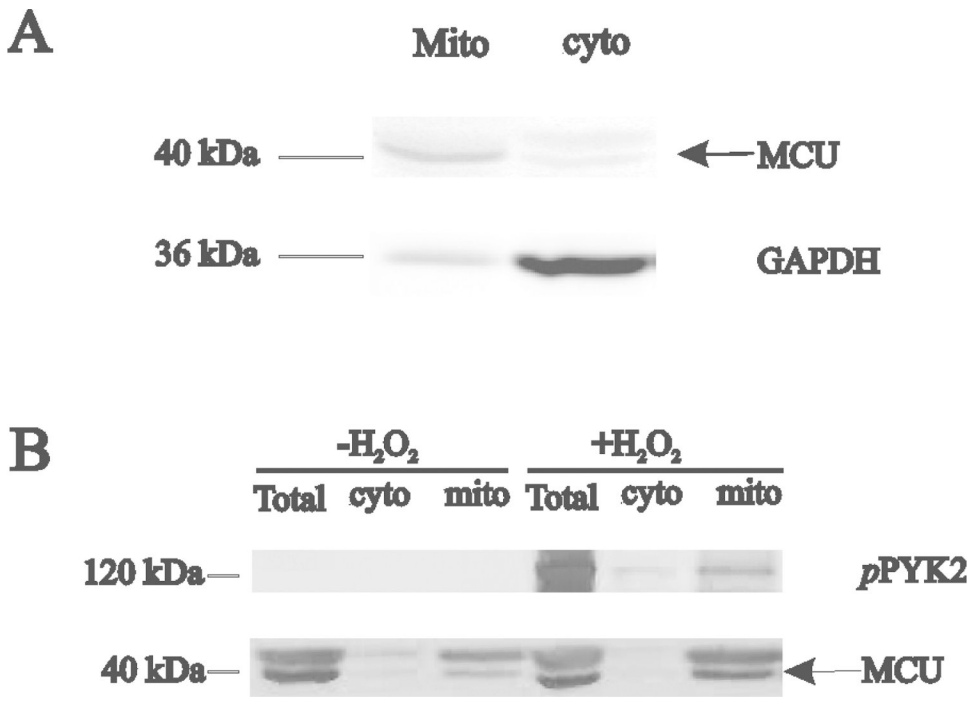

Figure 4. Trpm2 activation results in pPyk2 translocation to the mitochondria in adult cardiac myocytes.

A. LV myocytes from WT hearts were separated into cytosolic (GAPDH) and mitochondrial (MCU, mitochondrial Ca^{2+} uniporter) fractions (Materials and Methods). B. LV myocytes isolated from WT hearts were exposed to vehicle or H_2O_2 (200 μM) for 15 min before subcellular fractionation. Representative blot of pPyk2, Pyk2 and MCU in homogenate (total), cytosolic (cyto) and mitochondrial (mito) fractions of 1 of 3 separate myocyte preparations.

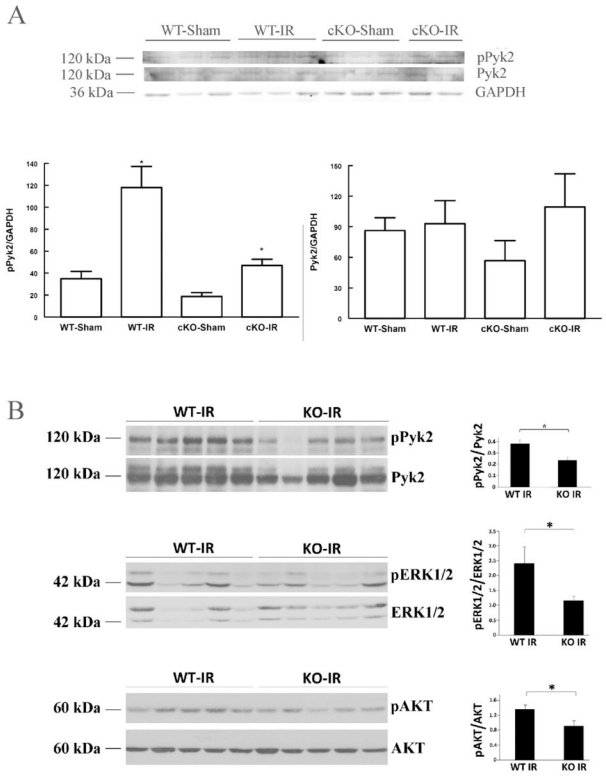

Figure 5. Trpm2 deficiency results in less pPyk2, pERK1/2 and pAkt after ischemia/reperfusion.

WT, cKO and gKO mice underwent sham operation or I/R surgery (30 min LAD ischemia, 72h reperfusion) (Materials and Methods) before heart homogenates were prepared for immunoblotting. A. Western blots of pPyk2, Pyk2 and GAPDH (loading control) from 3 WT-sham, 3 WT-I/R , 3 cKO-sham and 4 cKO-I/R (only 2 are shown) hearts. For pPyk2/GAPDH, *p<0.025, WT-sham vs. WT-I/R, cKO-sham vs. cKO-I/R, or WT-I/R vs. cKO-I/R. There are no statistically significant differences in total Pyk2/GAPDH among the 4 groups. B. Western blots of pPyk2, Pyk2, pERK1/2, ERK1/2, pAkt and Akt from 5 WT-I/R and 5 gKO-I/R hearts are shown on left, and summaries of fractional phosphorylation are shown on right. *p<0.05, WT-I/R vs. gKO-I/R.

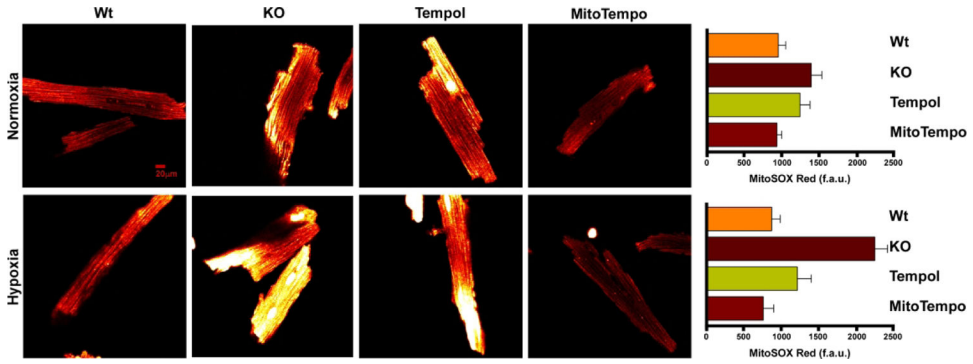

Figure 6. MitoTempo and Tempol decreases elevated $O_2^{\cdot -}$ levels in gKO myocytes after hypoxia/reoxygenation.

Global Trpm2 KO myocytes were pre-incubated with MitoTempo (50 nM) or Tempol (100 μM) or vehicle for 60 min before subjected to 30 min of normoxia (21% O_2-5% CO_2) or hypoxia (1% O_2-5% CO_2) followed by 30 min of reoxygenation. During reoxygenation, myocytes were loaded with the mitochondrial $O_2^{\cdot -}$ sensitive fluorophore MitoSOX Red (Materials and Methods). Representative confocal images are shown for WT, gKO, gKO-Tempol and gKO-MitoTempo after normoxic (upper panel) and H/R (bottom panel) incubations. There are 9 WT, 15 gKO, 15 gKO-Tempol and 15 gKO-MitoTempo myocytes incubated under normoxic conditions and 12 WT, 15 gKO, 12 gKO-Tempol and 15 gKO-MitoTempo myocytes incubated under hypoxic conditions followed by reoxygenation. Under normoxic conditions, there are no statistically significant differences in $O_2^{\cdot -}$ levels among WT, gKO, gKO-Tempol and gKO-MitoTempo myocytes although gKO myocytes tended to have higher $O_2^{\cdot -}$ levels compared to WT myocytes (Upper panel). After H/R, KO myocytes had significantly ($p<0.001$) higher superoxide levels than WT myocytes. Both MitoTempo and Tempol were effective in reducing the elevated $O_2^{\cdot -}$ levels in gKO-H/R myocyte ($p<0.001$ compared to gKO-H/R myocytes).

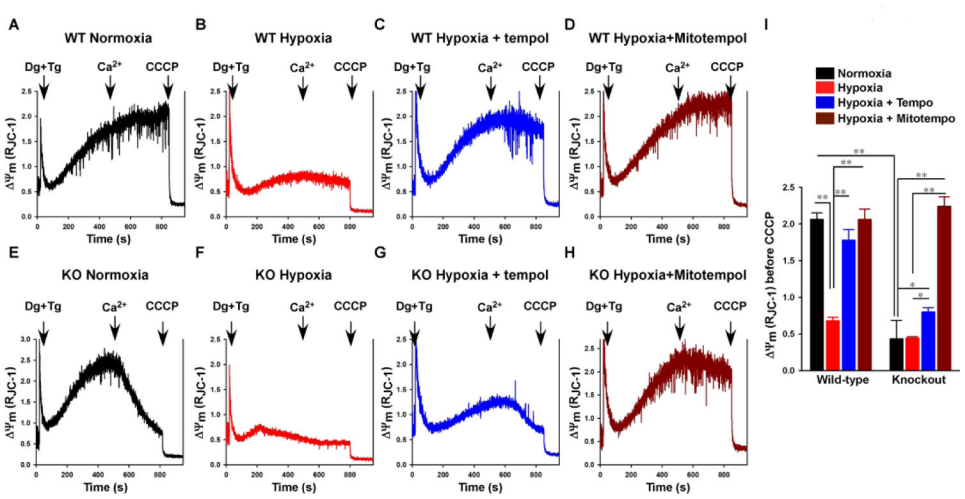

Figure 7. MitoTempo but not Tempol restores $\Delta\Psi_m$ in gKO myocytes after hypoxia/ reoxygenation.

Left: LV myocytes isolated from WT and gKO mice were pre-incubated with vehicle, MitoTempo (50 nM) or Tempol (100 μM) for 60 min, and then subjected to normoxia or hypoxia for 30 min followed by 30 min of reoxygenation. Myocytes were permeabilized with digitonin (Dg), treated with thapsigargin (Tg) and supplemented with succinate (Materials and Methods). The ratiometric $\Delta\Psi_m$ indicator JC-1 was used to measure $\Delta\Psi_m$. At times indicated (arrows), Ca^{2+} (10 μM) and the mitochondrial uncoupler CCCP were added. Right: Summary of $\Delta\Psi_m$ data from 3 separate myocyte preparations. *p<0.05; **p<0.01.

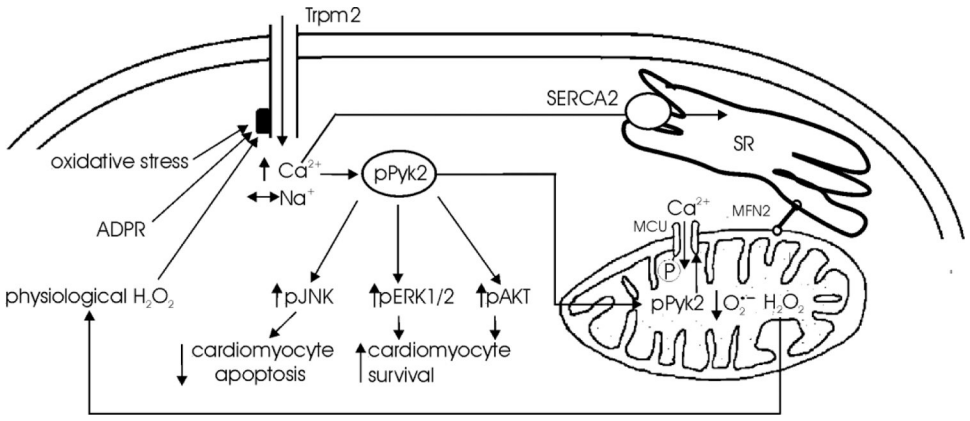

Figure 8. Schematic of the influence of Trpm2 on Pyk2 phosphorylation, mitochondrial Ca^{2+} uptake and function, ROS production, and cell survival.

Trpm2 in cardiac myocytes can be activated by physiological levels of H_2O_2 arising from mitochondrial respiration (Stanley, Sivakumaran et al. 2011), ADPR (Miller, Hoffman et al. 2014) and oxidative stress (e.g., exogenous H_2O_2). Activated Trpm2 channels are permeable to Ca^{2+} and Na^+ (Miller, Hoffman et al. 2014). In adult cardiac myocytes, $[Ca^{2+}]_i$ (Miller, Wang et al. 2013) but not $[Na^+]_i$ (Hoffman, Miller et al. 2015) is elevated with Trpm2 activation by H_2O_2. Some of the Ca^{2+} is taken up into the sarcoplasmic reticulum (SR) by SR Ca^{2+}-ATPase (SERCA2). Trpm2-mediated $[Ca^{2+}]_i$ increase results in Pyk2 phosphorylation (Figs. 1, 2 and 3). Phosphorylated Pyk2 translocates to the mitochondria (Fig. 4), resulting in phosphorylation of mitochondria Ca^{2+} uniporter (MCU), thereby accelerating mitochondrial Ca^{2+} uptake (O-Uchi, Jhun et al. 2014). Mitochondrial Ca^{2+} stimulates Ca^{2+}-sensitive Krebs cycle dehydrogenases (McCormack and Denton 1980), making available NADH and $FADH_2$ for the electron transport chain (Chen, Csordas et al. 2012), and assuring efficient electron flow during oxidative phosphorylation, both for bioenergetics maintenance and to ensure that physiological but not toxic levels of ROS are generated (Kohlhaas, Liu et al. 2010). Mitofusin-2 (MFN-2) which tethers the mitochondria to SR/ER (de Brito and Scorrano 2008, Chen, Csordas et al. 2012) allows efficient transfer of Ca^{2+} from ER/SR to mitochondria. In addition, Trpm2 regulates Complex I and Complex IV levels in the mitochondria (Miller, Hoffman et al. 2014, Hoffman, Miller et al. 2015). All these diverse effects of Trpm2 act in concert to maintain mitochondrial membrane potential, mitochondrial Ca^{2+} uptake, oxygen consumption rate, ATP levels and to minimize toxic levels of ROS (Miller, Hoffman et al. 2014). Trpm2-mediated Pyk2 phosphorylation promotes downstream pro-survival signaling pathways such as Akt and ERK1/2 (Fig. 5) (Yamamoto, Shimizu et al. 2008) and reduces apoptosis via JNK activation (Dougherty, Kubasiak et al. 2004).